

The Correspondence between Sudden Commencements and Geomagnetically Induced Currents; Insights from New Zealand

A. W. Smith¹, C. J. Rodger², D. H. Mac Manus², C. Forsyth¹, I. J. Rae³, M. P. Freeman⁴, M. A. Clilverd⁴, T. Petersen⁵, M. Dalzell⁶

¹Mullard Space Science Laboratory, UCL, Dorking, UK

²Department of Physics, University of Otago, Dunedin, New Zealand

³Department of Mathematics, Physics and Electrical Engineering, Northumbria University, Newcastle

upon Tyne, UK

⁴British Antarctic Survey, Cambridge, UK

⁵GNS Science, Wellington, New Zealand

⁶Transpower New Zealand Limited, Wellington, New Zealand

Key Points:

- The rate of change of the magnetic field during Sudden Commencements excellently correlates with observed Geomagnetically Induced Currents.
- Storm Sudden Commencements are associated with 22% larger GICs than Sudden Impulses.
- Sudden Commencements that occur when New Zealand is on the dayside of the Earth are associated with 30% larger GICs.

Corresponding author: A. W. Smith, andy.w.smith@ucl.ac.uk

This article has been accepted for publication and undergone full peer review but has not been through the copyediting, typesetting, pagination and proofreading process, which may lead to differences between this version and the [Version of Record](#). Please cite this article as doi: [10.1029/2021SW002983](https://doi.org/10.1029/2021SW002983).

This article is protected by copyright. All rights reserved.

Abstract

Variability of the geomagnetic field induces anomalous Geomagnetically Induced Currents (GICs) in grounded conducting infrastructure. GICs represent a serious space weather hazard, but are not often measured directly and the rate of change of the magnetic field is often used as a proxy. We assess the correlation between the rate of change of the magnetic field and GICs during Sudden Commencements (SCs), at a location in New Zealand. We observe excellent correlations ($r^2 \sim 0.9$) between the maximum one-minute rate of change of the field and maximum GIC. Nonetheless, though SCs represent a relatively simple geomagnetic signature, we find that the correspondence systematically depends on several factors. If the SC occurs when New Zealand is on the day-side of the Earth then the magnetic changes are linked to 30% greater GICs than if New Zealand is on the nightside. We investigate, finding that the orientation of the strongest magnetic deflection is important: changes predominantly in the east-west direction drive 36% stronger GICs. Dayside SCs are also associated with faster maximum rates of change of the field at 1 s resolution. Therefore, while the maximum rates of change of the magnetic field and GICs are well correlated, the orientation and sub-one-minute resolution details of the field change are important to consider when estimating the associated currents. Finally, if the SC is later followed by a geomagnetic storm then a given rate of change of the magnetic field is associated with 22% larger GICs, compared to if the SC is isolated.

Plain Language Summary

Changes in the Earth's magnetic field will drive electrical currents that can flow in infrastructure such as power networks and pipelines. These currents can pose a hazard to their operation and safety. We often do not have access to direct measurements of the currents that flow within our infrastructure, so we typically report and forecast magnetic perturbations to infer when we are likely to see large currents. In this work we investigate the link between the magnetic changes and currents that are observed when the Earth is impacted by a sharp change in the solar wind dynamic pressure, i.e. a shock. We also have access to direct measurements of current in infrastructure from New Zealand. In general we find excellent correlations between the two parameters. However, we find that the type of shock event during which they are observed is important, as is the location of the observations relative to the day/nightside of the Earth. We find that the orientation of the rate of change of the magnetic field as well as high time resolution (i.e. sub minute resolution) information are both important to consider when attempting to estimate the currents that will be generated, even with relatively simple processes.

1 Introduction

Rapid changes in the Earth's surface magnetic field generate anomalous currents in large scale grounded infrastructure, these are known as Geomagnetically Induced Currents (GICs). Examples of infrastructure vulnerable to GICs includes pipelines, power networks and railways. In such systems GICs can cause increased weathering of components, or in extreme cases even direct damage (e.g. Boteler et al., 1998; Boteler, 2021; Liu et al., 2016; Rajput et al., 2020). Power networks are particularly vulnerable to the effects of large GICs, as these can damage transformers and cause blackouts (e.g. Bolduc, 2002; Beland & Small, 2004; Gaunt & Coetzee, 2007; Eastwood et al., 2018). Some of the risks - and ultimately economic costs - associated with the generation of large GICs can be mitigated provided sufficient warning (Oughton et al., 2019), making forecasting such intervals a critical endeavor. However, the ability to provide accurate forecasts relies on our understanding of the dynamic interactions between the solar wind and magnetosphere, as well as how those processes couple to the solid Earth.

69 Direct measurements of GICs are relatively sparse, and are rarely available for suf-
70 ficiently long intervals to permit detailed statistical study. Therefore studies that require
71 long baselines often use the rate of change of the surface magnetic field as a proxy mea-
72 surement (e.g. Viljanen et al., 2001; Thomson et al., 2011; Carter et al., 2015; Freeman
73 et al., 2019; Smith et al., 2019; Smith, Forsyth, Rae, Rodger, & Freeman, 2021). Such
74 magnetic field measurements are comparatively plentiful, and are readily available for
75 many locations across the globe, with records spanning decades. In general, excellent cor-
76 relations have been observed between the magnitude of GICs and the rate of change of
77 the local magnetic field (e.g. Mac Manus et al., 2017; Rodger et al., 2017; Zhang et al.,
78 2020). However, the precise translations between the magnetic field changes and observed
79 GICs are complex. Physically, the time-varying geomagnetic field will induce a geoelec-
80 tric field in the ground, it is then the strength and relative direction of the geoelectric
81 field that will determine the GICs that result in the grounded infrastructure. Full mod-
82 eling of such a process requires knowledge of the direction, strength and frequency con-
83 tent of the magnetic field changes, as well as the local geology and the geometry and prop-
84 erties of the local power networks (Thomson et al., 2005; Viljanen et al., 2013; Beggan
85 et al., 2013; Beggan, 2015; Divett et al., 2018; Blake et al., 2018; Dimmock et al., 2019;
86 Divett et al., 2020; Cordell et al., 2021; Mac Manus et al., 2022). Unfortunately, detailed
87 3D conductivity models are not available for many locations across the globe.

88 A wide range of dynamical processes in near-Earth space can cause rapid magnetic
89 fluctuations on the ground (e.g. Rogers et al., 2020) and consequently GICs (e.g. Kap-
90 penman, 2005; Clilverd et al., 2018; Tsurutani & Hajra, 2021). In particular large mag-
91 netic field changes and GICs are often associated with geomagnetic storms and substorms
92 (e.g. Eastwood et al., 2017; Ngwira et al., 2018; Freeman et al., 2019; Dimmock et al.,
93 2019), during which strong and dynamic ionospheric currents are generated. These iono-
94 spheric currents vary over relatively short spatial scales (e.g. Murphy et al., 2013; Forsyth
95 et al., 2014; Pulkkinen et al., 2015), and are therefore challenging to forecast. The pic-
96 ture is further complicated by considerable spatial variations in local ground conductiv-
97 ity. These factors combine to result in large differences in observed GICs over spatial scales
98 of 100s of kilometers or less (e.g. Ngwira et al., 2015; Bedrosian & Love, 2015; Mac Manus
99 et al., 2017; Dimmock et al., 2020).

100 Sudden Commencements (SCs) are another key magnetospheric phenomenon that
101 can generate large magnetic field changes (Fiori et al., 2014; D. M. Oliveira et al., 2018;
102 D. Oliveira & Samsonov, 2018; Smith et al., 2019; Smith, Forsyth, Rae, Rodger, & Free-
103 man, 2021) and consequently GICs (Kappenman, 2003; Pulkkinen et al., 2005; Marshall
104 et al., 2012; Zhang et al., 2015; Carter et al., 2015). SCs are impulsive phenomena caused
105 by the impact of a large increase in solar wind dynamic pressure on the magnetosphere,
106 i.e. a solar wind shock (Takeuchi et al., 2002; Lühr et al., 2009). Critically for forecast-
107 ing purposes, solar wind shocks represent a distinct and coherent phenomenon that are
108 observable upstream of the Earth at L1 prior to impact (e.g. Cash et al., 2014). They
109 also often precede further magnetospheric activity, i.e. geomagnetic storms and substorms
110 (Akasofu & Chao, 1980; Gonzalez et al., 1994; Zhou & Tsurutani, 2001; Yue et al., 2010).
111 Consequently, while SCs themselves may not be responsible for large portions of extreme
112 magnetic variability, the interval of time that follows can account for 90% of extreme mag-
113 netic field variability (Smith et al., 2019; Smith, Forsyth, Rae, Rodger, & Freeman, 2021),
114 at latitudes below 60°.

115 Recent space weather modelling efforts have produced models that can skillfully
116 forecast the rate of change of the magnetic field to provide advance warning of GICs (e.g.
117 Wintoft et al., 2015; Keese et al., 2020; Camporeale et al., 2020; Smith, Forsyth, Rae,
118 Garton, et al., 2021), with the implicit assumption that large rates of change of the mag-
119 netic field will generate large GICs (Viljanen et al., 2001). However, as outlined above,
120 the relationship between the rate of change of the magnetic field and GICs is complex
121 and depends on many local factors, with accurate translation requiring careful modelling

(e.g. Divett et al., 2018; Blake et al., 2018; Mac Manus et al., 2022). The necessary detailed geophysical models are often not available, and so in this work we assess the relationship between the rate of change of the magnetic field and GICs during the simplest of magnetospheric drivers in order to provide an estimate of the uncertainty inherent in assuming such a correlation, as well as investigating factors that impact the relationship between the rate of change of the field and GICs. The South Island of New Zealand presents an excellent opportunity to study the correlation between the rate of change of the magnetic field and GICs (e.g. Mac Manus et al., 2017; Rodger et al., 2017, 2020; Clilverd et al., 2018, 2020). For over a decade contemporaneous magnetic field and GIC measurements have been made in close geographical proximity.

2 Data

In this study we consider the period between the years 2001 to 2016. During this time magnetic field data are available from the Eyrewell (EYR) magnetometer station, along with complementary GIC data from the nearby Islington (ISL) substation, transformer number 6 in particular. Figure 1 provides a geographical overview of the locations of both the EYR magnetometer station and the ISL transformer on the South Island of New Zealand. It is clear from Figure 1 that the nearby coast of New Zealand is predominantly in the NE-SW direction, while the majority of the long distance power lines in the South Island are similarly oriented, though north of ISL the lines run much closer to N-S. For a more detailed description of the New Zealand power network we direct the interested reader to Mac Manus et al. (2017).

The GIC data from the ISL transformer number 6 have been selected for two main reasons. First, this transformer is geographically close (< 20 km) to the EYR magnetometer station, such that the comparison of the rate of change of the magnetic field and GIC measurements will be valid. Second, of the GIC data available from New Zealand's South Island, this data is available for the longest period of time, permitting the most extensive statistical analysis. A detailed description of the instrumentation and method by which the GIC component may be identified in the raw data can be found in Mac Manus et al. (2017). As described by Clilverd et al. (2020), while the nominal resolution of the data is 4 s, the data are compressed such that data are not recorded if the change from the last record is less than 0.2 A. Thus some measure of decompression is required. This variable resolution predominantly impacts data obtained during geomagnetically quiet intervals, when the GIC levels are consistent. We use the uncompressed 4 s data for this study.

For the majority of this study we use 60 s resolution data from the EYR magnetometer station. This resolution is sufficient for the identification and preliminary examination of SCs, having been shown to well correlate with recorded GICs (Mac Manus et al., 2017; Rodger et al., 2017). For the final investigation in this study the limitations of the one-minute resolution data are investigated. For this examination 1 s resolution data are used, though we note that this data is available for only a limited fraction of the study period, as discussed in Section 4.1.2.

To investigate SCs we use the SOHO interplanetary shock list produced by the ShockSpotter procedure (<http://umtof.umd.edu/pm/>). In total 404 shocks were observed in the interval considered by this study. The time of the shock impact on the magnetosphere, and resulting SC, were identified manually through inspection of the magnetic field at the EYR station. Of the 404 interplanetary shocks, a total of 329 possess both the necessary magnetic field and GIC data at the shock arrival time, and therefore form the basis of this work.

If SCs are followed by a geomagnetic storm then they may be termed a Storm Sudden Commencement (SSC), while if they are not then they may be called a Sudden Im-

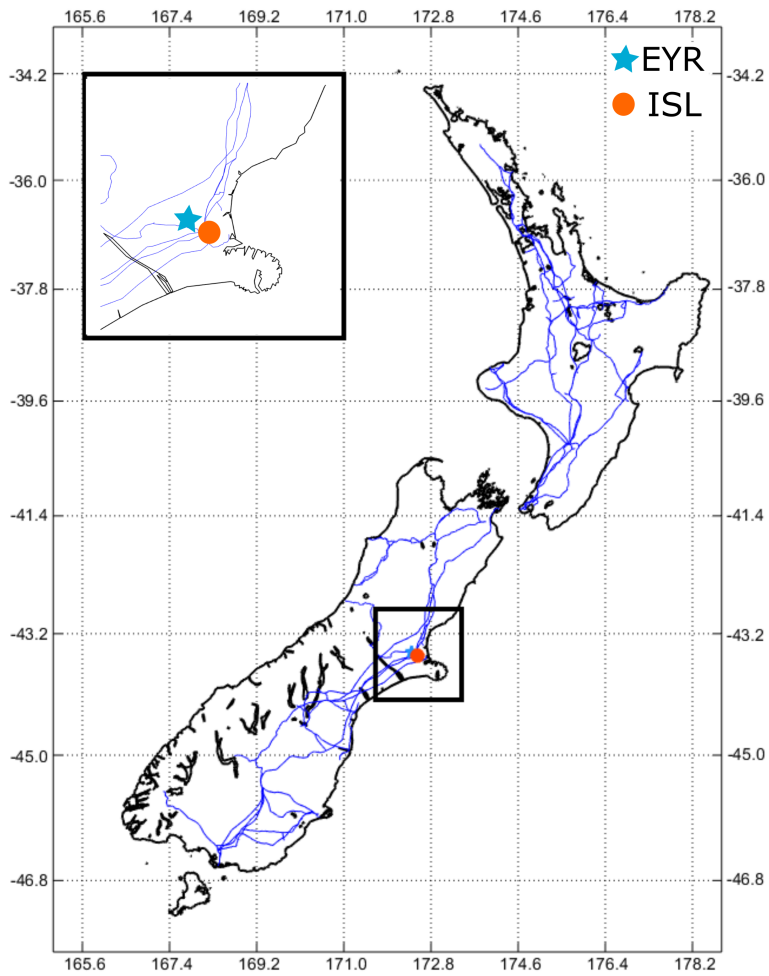


Figure 1. Map of New Zealand showing the location of the Eyrewell (EYR) magnetometer station (blue star) and the Islington (ISL) substation (orange circle). Transmission lines are indicated in blue.

172 pulse (SI). To evaluate this classification we use the Sym-H index in the 24 hours fol-
 173 lowing the SC. If the Sym-H index drops to less than -50 nT in this time, then it is clas-
 174 sified as an SSC. This definition does not include any consideration of the “changing mag-
 175 netic rhythm” criterion that is sometimes used to identify SSCs (Mayaud, 1973), how-
 176 ever it is easily reproducible. In total the 329 SCs can be subdivided into 145 SSCs and
 177 184 SIs.

178 In a recent study, Smith et al. (2020) showed that a skilful prediction can be made
 179 as to whether an observed solar wind shock will cause an SC, or will precede a geomag-
 180 netic storm (i.e. an SSC). The most powerful predictive parameter of the shock in de-
 181 termining whether it will cause an SC was found to be the range in the interplanetary
 182 magnetic field strength ($|B|$) over the shock. Meanwhile, the minimum value of the north-
 183 south component of the interplanetary magnetic field (i.e. the minimum B_z) was found
 184 to be the most powerful parameter in forecasting whether a given shock would be related
 185 to an SSC.

186 3 Results

187 First, we present a statistical overview of the rate of change of the horizontal ground
 188 magnetic field (H') and GICs around the 329 SC events. Figure 2 shows Superposed Epoch
 189 Analyses of the one-minute rate of change of the horizontal magnetic field (H') at the
 190 EYR magnetometer station (Figure 2a) and the GIC measured at the nearby ISL M6
 191 transformer (Figure 2b). The zero epoch is defined as the time at which the shock im-
 192 pact was seen in the EYR magnetometer data, i.e. the start of the SC signature at this
 193 location.

194 Prior to the SCs we can see that the rate of change of the magnetic field at EYR
 195 is low, with a median of around $0.25-0.3$ nTmin $^{-1}$. These likely represents background
 196 field changes. In the same interval we see small GICs at ISL, with values of $0.1-0.2$ A.
 197 At the SC itself we see significant increases in the rate of change of the magnetic field,
 198 with a median of 5 nTmin $^{-1}$, and the measured GIC at ISL, with a median of ~ 0.7 A.
 199 In the day that follows the SCs we do not see any clear impulsive signatures in the rate
 200 of change of the magnetic field or GIC, however the median and quartiles are both el-
 201 evated. For example, the upper quartile of the measured GIC is around 0.5 A, approx-
 202 imately twice as large as before the SC. This suggests that magnetospheric activity is
 203 occurring, possibly related to geomagnetic storms and substorms for some SCs, though
 204 it is aliased in time relative to the SC and so is not coherently recorded in the median
 205 of all events.

206 For context, Mac Manus et al. (2017) found that GICs greater than 5 A represented
 207 “significant” GICs in the South island of New Zealand, with peak GICs of between 20
 208 and 50 A being observed during large geomagnetic storms. It has been estimated that
 209 a GIC of ~ 100 A during a geomagnetic storm in November 2001 caused transformer
 210 failure in Dunedin (Rodger et al., 2017). Nonetheless, Rodger et al. (2020) showed clear
 211 evidence of transformer saturation (through observed harmonic distortion) for much lower
 212 levels of GIC.

213 We now zoom into the rate of change of the magnetic field observed during the SC
 214 itself, i.e. the few minutes around epoch zero in Figure 2. An SC will represent as close
 215 to an impulsive driver as can be found in the magnetosphere, though the magnetic field
 216 signature will still contain different components (e.g. Araki, 1994). Figure 3 investigates
 217 the correlation between the largest observed rate of change of the magnetic field at EYR
 218 (H') and the largest measured GIC at ISL during the SCs. In this work we consider a
 219 window from -30 s before “Epoch 0” till 150 s afterwards. This window has been se-
 220 lected to account for any delays due to the inductance of the power system. The full com-

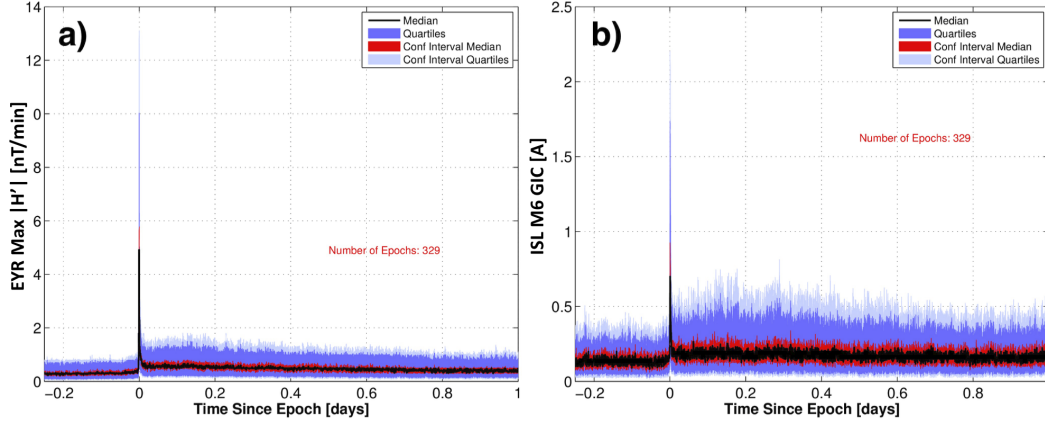


Figure 2. Superposed Epoch Analyses (SEAs) of the rate of change of the horizontal magnetic field (a) and observed GIC (b) from 0.25 days before 329 SCs, through to 1 day after the SCs. Epoch 0 is defined as the time of shock impact, i.e. the start of the SC, in the EYR magnetometer data. The black and red show the median and associated confidence interval, while the blue and light blue show the quartiles and associated confidence intervals.

221 plement of 329 SCs is shown in Figure 3a, while the SSC and SI subsets are shown in
 222 Figures 3b and c.

223 Overall, Figure 3 shows excellent correlations between the measured H' at EYR
 224 and GIC at ISL, with the r^2 values of ~ 0.9 for the SC and SSC subsets. The SI events
 225 show a slightly lower r^2 of ~ 0.8 . We have performed a linear fit to the data, using or-
 226 thogonal distance regression, producing the red dashed lines. These linear fits are con-
 227 strained to have a constant of zero (i.e. to pass through the origin), however we note that
 228 this choice did not materially change the results. The gradient of the fit is provided in
 229 the top left of the panels, labeled 'm'. For the full catalog of SCs, we find a gradient of
 230 $0.208 \text{ A nT}^{-1}\text{min}$. This gradient is slightly larger for the SSC subset (at $0.214 \text{ A nT}^{-1}\text{min}$),
 231 and reduced for those events classified as SIs (at $0.175 \text{ A nT}^{-1}\text{min}$). This amounts to
 232 a 22% larger gradient for SSC-type events, and therefore a given rate of change of the
 233 magnetic field caused by an SSC would be expected to generate a 22% larger current when
 234 contrasted with an SI. These gradients are statistically significantly different: $p < 0.01$,
 235 suggesting that the null hypothesis - that the gradients are in fact the same - can be re-
 236 jected with a false positive risk of less than 1%. However, Figure 3 also shows that the
 237 majority of SCs are clustered in the lower left corner, at low values of H' and GIC, i.e.
 238 less than $\sim 3 \text{ A}$ and $\sim 15 \text{ nTmin}^{-1}$.

239 One factor that could explain some of the scatter in Figure 3 is that the orienta-
 240 tion of the magnetic field change is not the same for every SC. A different orientation
 241 of rate of change of the field would result in differential interaction with the local geol-
 242 ogy, impacting the geoelectric field generated and thus the GICs measured. This would
 243 provide a degree of systematic scatter. It is known that the ground signature of an SC
 244 can vary with both longitude and latitude (e.g. Araki, 1994; Moretto et al., 1997), though
 245 for this study the latitude is fixed by the choice of location. Figure 4 shows the direc-
 246 tion of the strongest magnetic field change measured at EYR during the SCs. We can
 247 see that though most of the deflections are towards the center of Figure 4, and are there-
 248 fore mostly in the northward direction, there are a number of very large deflections that
 249 are directed southward. These anomalously directed magnetic field deflections are mostly
 250 found in the noon and dawn sectors, and almost all of the largest deflections in these sec-
 251 tors show similar directionality. Therefore, limiting the analysis to a sector of local time

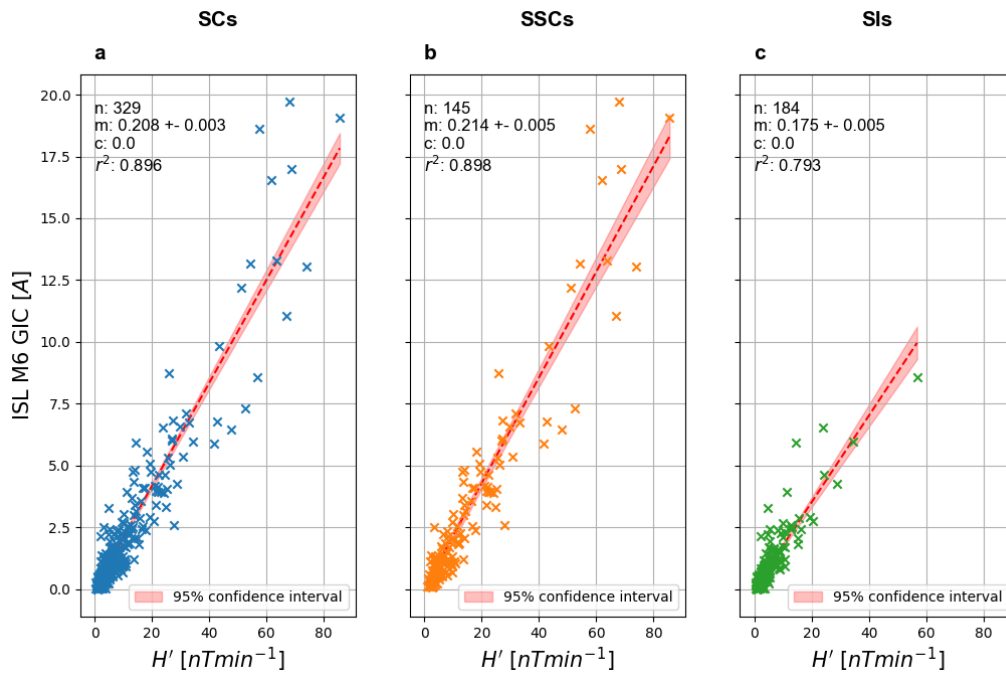


Figure 3. Scatter plots showing the correlation between H' at EYR and the GIC measured at ISL. The plots are shown for all 329 SCs (a), 145 SSCs (b) and 184 SIs (c). The red dashed line indicates the best linear fit to the data, constrained to go through the origin. The red shaded region indicates the 95% confidence interval, while the best-fit parameters (n: number, m: gradient, c: intercept) are provided with their 1σ limits. The intercepts of the fits are constrained to be zero.

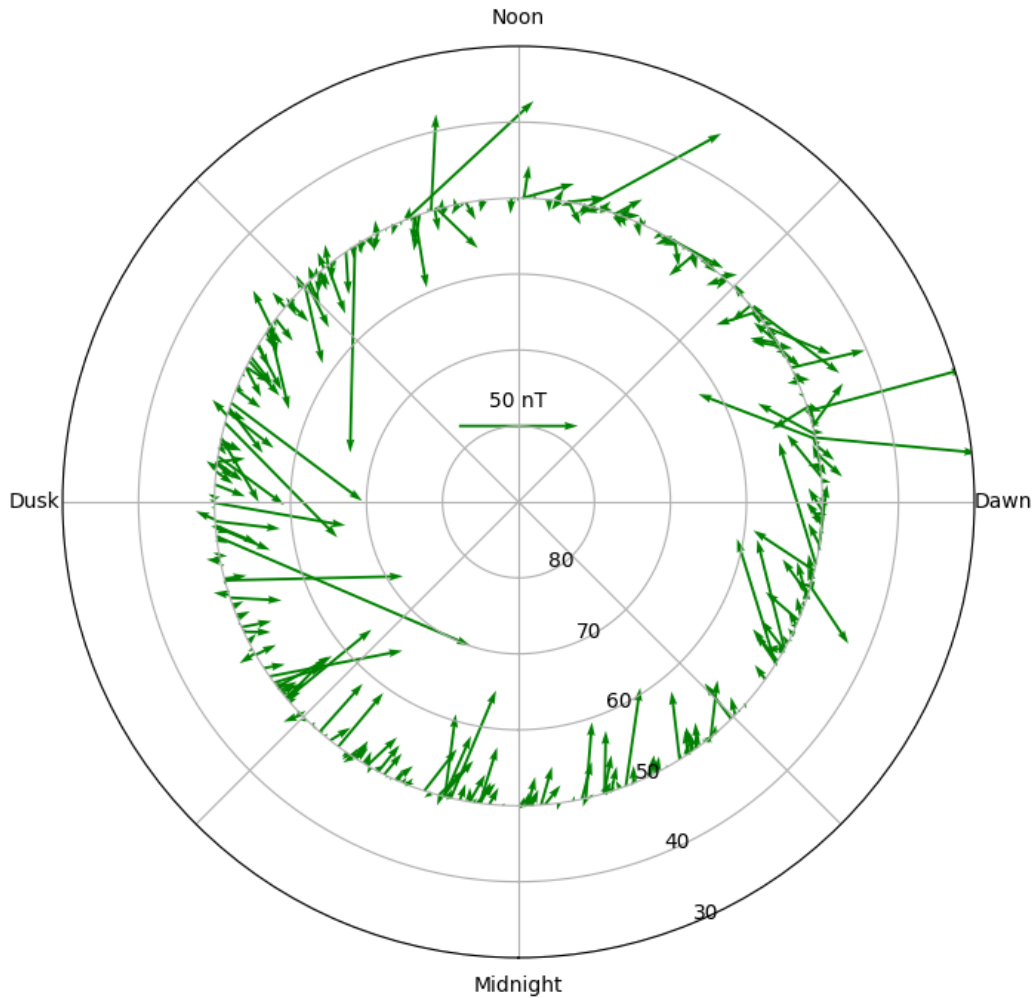


Figure 4. Quiver diagram demonstrating the directionality of the largest rate of change of the magnetic field during SCs as a function of local time, viewed from above the Earth looking down. Quiver length is proportional to the magnitude of the rate of change of the field, with the key in the middle representing 50 nTmin^{-1} . The base of each quiver is at the local time of New Zealand at the start of the SC, while the latitude is fixed at the latitude of New Zealand (50°). The direction of the quiver is such that a purely Northward rate of change of the field will be towards the center of the diagram.

will provide a test as to whether there is an orientation of large rates of change of the magnetic field that will generate a geoelectric field that will couple more strongly to the power network (i.e. a geoelectric field closely aligned with the local network).

Figure 4 indicates that there may be a local time dependence of the orientation of the strong magnetic deflections, and so as a first test we can examine the correlations shown in Figure 3, but subdivided by the Magnetic Local Time (MLT) of New Zealand. Figure 5 shows the correlations between the rate of change of the magnetic field and the observed GIC, split according to whether the magnetic local time of the EYR magnetometer station was on the day- (top row) or night-side (bottom row) of the Earth (split at 0600 and 1800 MLT). The majority of the correlations displayed in Figure 5 are higher

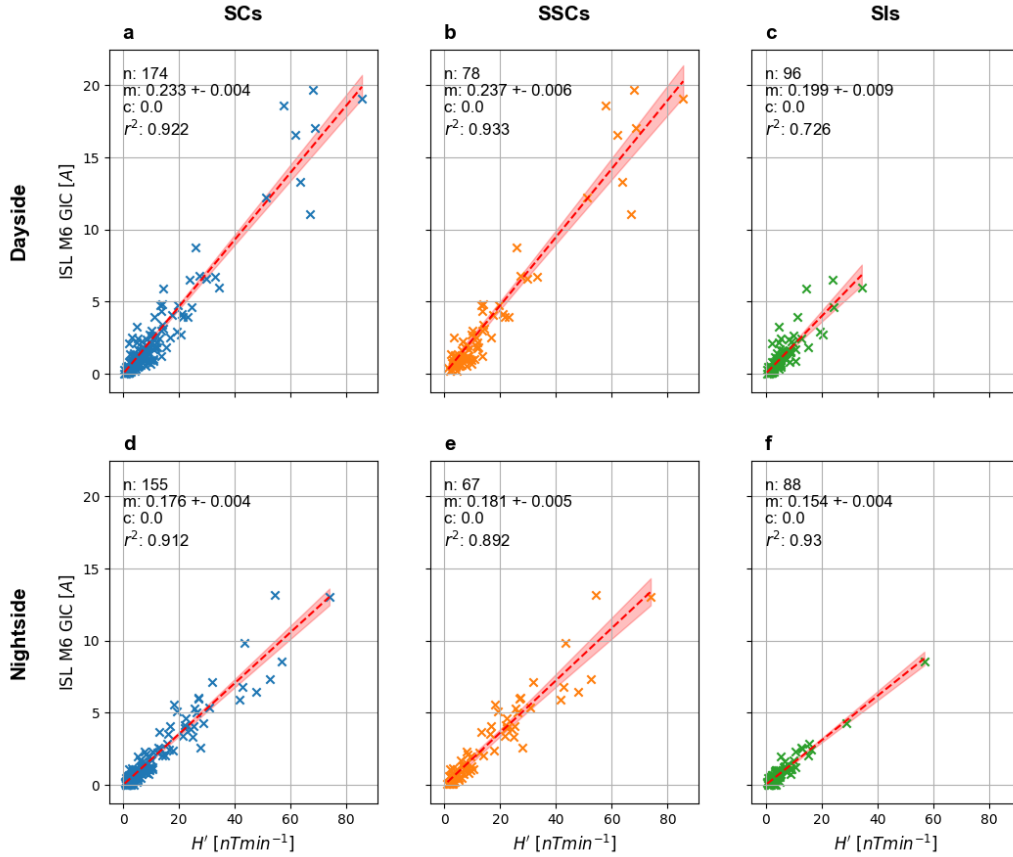


Figure 5. Scatter plots showing the correlation between H' at EYR and the GIC measured at ISL, split by the MLT of EYR during the SC. The top row (a - c) shows those events that occurred when EYR was on the dayside, i.e. between 0600 and 1800 MLT, while the bottom row (d - f) shows that occurred when EYR was on the nightside, i.e. between 1800 and 0600 MLT. The plots are shown for all 329 SCs (a, d), 145 SSCs (b, e) and 184 SIs (c, f). The format is the same as for Figure 3.

than previously, mostly in excess of $r^2 = 0.9$. It is also apparent that the best-fit gradients are larger for those SCs that occur when New Zealand (along with EYR and ISL) is on the dayside of the Earth (top row of Figure 5). For example, SCs show a 32% larger gradient on the dayside (top left) compared to the nightside (bottom left). This pattern is seen for both the SSC and SI subsets, at approximately 30% differences. These differences are highly statistically significant ($p \ll 0.01$). As in Figure 3, the SI type events show smaller gradients. It is interesting to note that a dayside SI (Figure 5c) shows a gradient that is slightly in excess of a nightside SSC event (Figure 5e). The different gradients are important as it suggests that some of the scatter evident in the correlation between the rate of change of the magnetic field and GIC (e.g. Figure 3) is related to the local time of the observations. For ISL transformer number 6, this would lead to up to a 30% discrepancy in predicted GIC, should a simple linear conversion be used to translate between the rate of change of the magnetic field and GIC. We note that if the local time bins are reduced, such that they now only cover two hours either side of noon and midnight, then the difference between the day and night side events is increased to a 60% difference in gradient (see Figure A1).

As noted above, the majority of SCs are clustered in the lower left corners of the plots, i.e. at low values of H' and GIC. We therefore examine whether the overall fitting results are impacted by the presence of few, extreme H' events which perhaps evoke a distinct result, i.e. we test the gradients of the correlation if only “small” H' events are considered. If we only consider SCs with $H' < 20$ nTmin⁻¹ then the gradients returned for the day and night subsets are 0.207 ± 0.007 A nT⁻¹min and 0.184 ± 0.006 A nT⁻¹min, respectively. This is a 12.5% difference, much less than was recovered with the full catalog (32%). For an SC associated with a rate of change of the magnetic field of 20 nTmin⁻¹ this would correspond to a difference in predicted GIC of < 0.5 A. Though the difference in gradient is statistically significant ($p < 0.01$), this raises the question as to whether this distinction for “small” (i.e. $H' < 20$ nTmin⁻¹) events would be of practical significance.

To summarize the findings thus far, we have shown a statistical increase in both the rate of change of the magnetic field and GIC during SCs, at EYR and ISL respectively. During SCs the majority of events show small rates of change of the magnetic field and GICs, i.e. less than ~ 3 A and ~ 15 nTmin⁻¹. Nonetheless, we have shown excellent correlations between the measured maximum rate of change of the magnetic field at EYR and GICs measured at ISL transformer number 6 during SCs (Figure 3). We have also investigated several potential sources of systematic scatter, and therefore uncertainty, in the correlation between the rate of change of the magnetic field and GICs. We have shown that - for the locations in the study - a given rate of change of the magnetic field that is associated with SSC-type events appears to more effectively generate GICs, such that a given rate of change of the magnetic field is linked to a 22% larger GIC (Figure 3). Also, when New Zealand is on the dayside of the planet a given rate of change of the magnetic field will generate a $\sim 30\%$ larger GIC, compared to when New Zealand is on the nightside of the planet (Figure 5). We will now investigate the reasons behind these findings, and discuss the implications for space weather forecasting and mitigation.

4 Discussion

4.1 The Correlation Between the Rate of Change of the Magnetic Field and GICs

The results above raise an important question: why are the GICs at ISL (for a given rate of change of the magnetic field at EYR) larger during SSC-type events, or during those SCs that occur when the location is on the dayside of the Earth? To translate a given rate of change of the magnetic field to a GIC there are several key parameters. A critical consideration is the direction of the induced geoelectric field with respect to the conducting network. Therefore, the conductivity of the local geology is fundamentally important (e.g. Bedrosian & Love, 2015; Beggan, 2015; Dimmock et al., 2019; Cordell et al., 2021), as it will determine the direction and strength of the geoelectric field generated by a given rate of change of the magnetic field. The second important parameter is the geometry and properties of the power network (e.g. Beggan et al., 2013; Blake et al., 2018; Divett et al., 2018, 2020). However, for the comparisons performed above these factors are identical as the location and power network considered are the same throughout. This suggests that the parameterization of each SC by the maximum one-minute rate of change of the magnetic field may be losing important information. There are two important factors that this parameterization neglects: the frequency content and the full directional vector of the SC magnetic signature. Both of these factors may depend on the MLT at which the SC is observed, and also on the way in which the solar wind has coupled to the magnetosphere.

While SCs are one of the most simple magnetic field signatures seen on the ground, it is known that the signature varies with magnetic local time and latitude. Empirically for example, the magnetic perturbations associated with SCs have been found to increase

in size moving away from the equatorial latitudes (Fiori et al., 2014; Smith, Forsyth, Rae, Rodger, & Freeman, 2021). At low latitudes the signature is dominated by a compressional perturbation related to the enhancement of the magnetopause current, sometimes known as the DL component (the disturbance dominant at low latitudes) (Araki, 1994). For a given solar wind shock, the DL perturbation is largest at noon local time and decreases towards midnight (Kokubun, 1983; Russell et al., 1992). Meanwhile, above a magnetic latitude of $\sim 30^\circ$ the DP component becomes significant. The DP component (the disturbance due to polar ionospheric currents) is caused by the coupling of the magnetospheric compression to shear Alfvén waves (Southwood & Kivelson, 1990), resulting in Traveling Convection Vortices (TCVs) in the ionosphere (Friis-Christensen et al., 1988). These TCVs propagate east and west away from the noon meridian, with strengths that maximize at around 0900 MLT (Moretto et al., 1997). Therefore, while SCs are often attributable to a distinct solar wind structure, there is some complexity involved in determining the nature of the precise ground signature that will be caused.

4.1.1 *Assessing the Orientation of the Rate of Change of the Magnetic Field*

To further examine these possibilities we will first assess the importance of the orientation of the magnetic signature observed at EYR. For this investigation we have split the SC signatures on the basis of whether the largest change in the magnetic field was predominantly in the geographical dX (north-south) or dY (east-west) direction. Figure 6 shows the correlation between the rate of change of the magnetic field and observed GIC for these subsets. It is clear that for most SCs the strongest deflection is predominantly in the north-south direction, with Figures 6a - c showing many more events than Figures 6d - f. This is to be expected, as at mid-latitudes the DL (compressional) component of the SC signature, is likely to dominate (Araki, 1994). The DL component is expected to be a mostly northward direction (albeit in a magnetic coordinate system). However, we see that the less numerous dY dominant events show much greater gradients in Figure 6, as seen in panels 6d - f. For SCs, we see a 36% larger GIC if the largest deflection is predominantly in the dY direction (Figure 6d compared to Figure 6a). This pattern is true regardless of whether the SC can be later defined as an SSC or SI. It therefore appears that SCs that contain a strong east-west magnetic field change may result in geoelectric fields that will couple better to the parts of the New Zealand power network that are pivotal for the ISL M6 transformer, reinforcing the importance of the full vector information of the magnetic field changes.

We showed that a similar difference in correlation is attributable to the location of the New Zealand observations in MLT, motivated by how the directionality of the largest rates of change of the magnetic field appear to depend on MLT (Figure 4). To check if these effects are distinct, Figure 7 shows the SCs split by the MLT of EYR as well as the orientation of the largest magnetic field deflection. As above, more SCs show the dX (north-south) dominance that would be expected of an SC with the DL component being the largest constituent of the magnetic signature. We also find that there are approximately twice as many dY dominant events observed on the dayside, compared to the nightside (43 compared to 23). Given that the magnetic latitude of the observatory is fixed, we could be seeing the result of the DP component varying in magnitude and/or direction with MLT. Indeed, the TCVs with which the DP component is associated are expected to propagate away from the noon meridian (Friis-Christensen et al., 1988), with the largest magnitudes found around 0900 MLT (Moretto et al., 1997). Our results would appear to be consistent with this interpretation.

As before, we see that dY dominant events show a larger gradient than the dX events, with remarkably high correlations. Those events for which dY dominates show 27–29% greater GIC values for a given maximum rate of change of the magnetic field. This is smaller than the differences we report above, but are highly statistically significant ($p <$

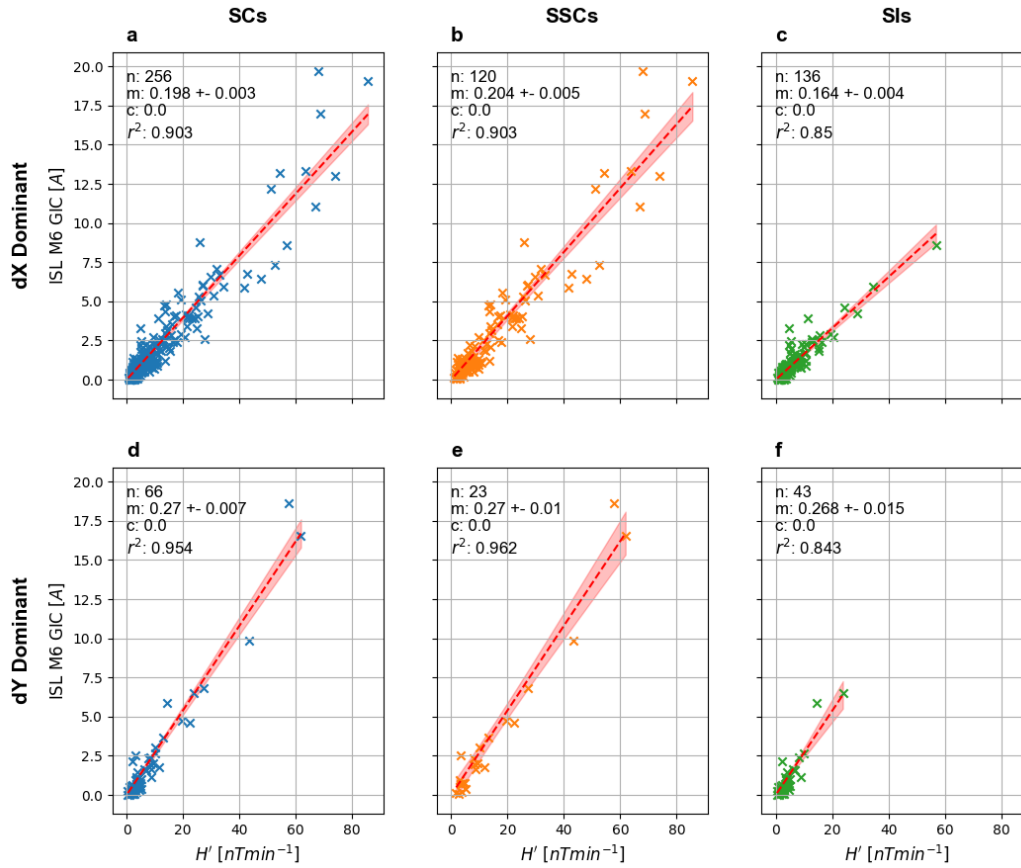


Figure 6. Scatter plots showing the correlation between H' at EYR and the GIC measured at ISL, split by the orientation of the largest rate of change of the magnetic field during the SC. The top row (a - c) shows those events for which the dX (north-south) deflection was dominant, while the bottom row (d - f) shows those events for which the dY (east-west) deflection was larger. The plots are shown for all SCs (a, d), SSCs (b, e) and SIs (c, f). The format is the same as for Figure 3 and 5.

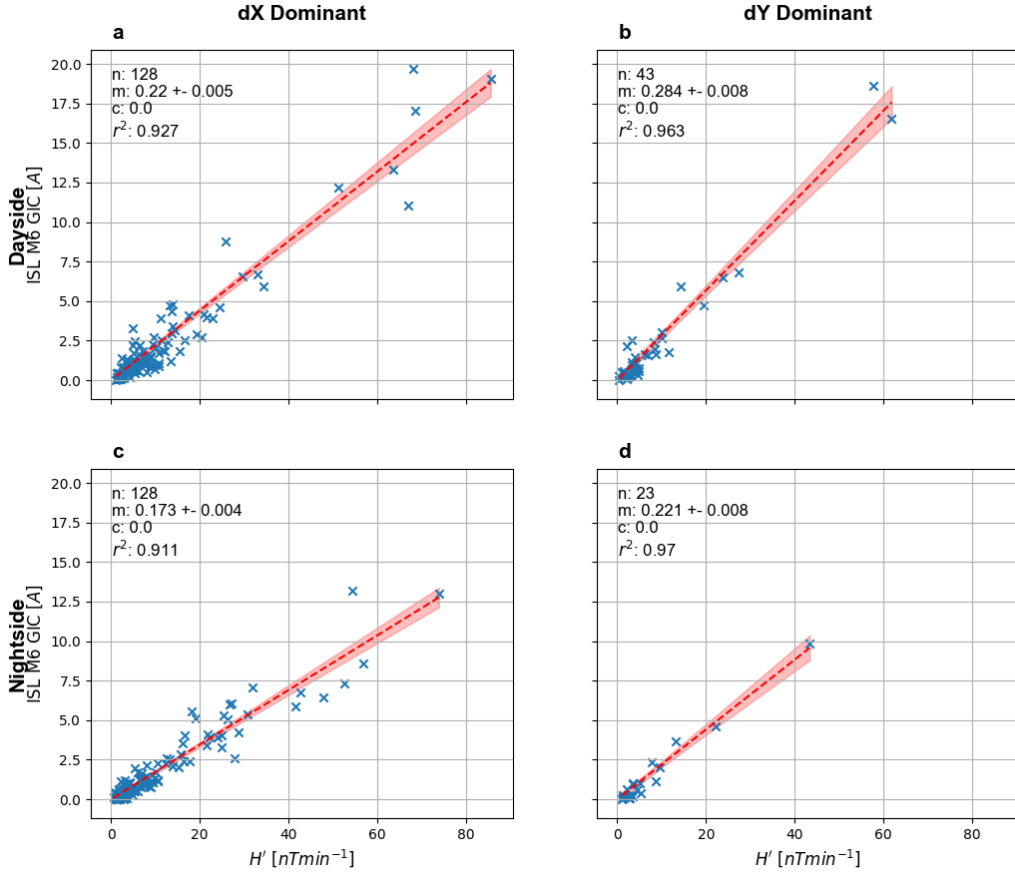


Figure 7. Scatter plots showing the correlation between H' at EYR and the GIC measured at ISL, split by the orientation of the largest rate of change of the magnetic field and MLT of ISL during the SC. The top row (a, b) shows those events that occurred when ISL was on the day side, i.e. between 0600 and 1800 MLT, while the bottom row (c, d) shows that occurred when ISL was on the night side, i.e. between 1800 and 0600 MLT. The left column (a, c) shows those events for which the dX (north-south) deflection was dominant, while the right column (b, d) shows those events for which the dY (east-west) deflection was larger. The format is similar to that in Figure 3.

0.01) given the small uncertainties in the gradients. We also still see a residual day/night effect in Figure 7, with dayside events showing 27–29% larger gradients. Interestingly, the effects combine such that nightside dY dominant events appear equivalent to dayside dX dominant events. This suggests that there are at least two distinct effects appearing in our data which are not solely the result of a directional dependence.

Table 1 shows the full results, including those for the SSC and SI subsets. The SSC subset are fully consistent with the relative differences reported above ($\sim 26\%$ differences in gradient), while the SI subset is less clear. The SI subset results could be less consistent due to the smaller number of SI events that show large rates of change of the field or GIC as these events dominate the gradients obtained. However, we do confirm that the largest gradients for all subsets are found for those events on the dayside, where the dY component is dominant.

SCs		
	dX Dominant	dY Dominant
Dayside	0.22 ± 0.005	0.284 ± 0.008
Nightside	0.173 ± 0.004	0.221 ± 0.008

SSCs		
	dX Dominant	dY Dominant
Dayside	0.225 ± 0.006	0.284 ± 0.011
Nightside	0.177 ± 0.006	0.225 ± 0.011

SIs		
	dX Dominant	dY Dominant
Dayside	0.177 ± 0.008	0.284 ± 0.017
Nightside	0.154 ± 0.004	0.156 ± 0.019

Table 1. Table of the gradients that result from performing the correlation analysis in Figure 7 on the SC, SSC and SI subsets.

4.1.2 Assessing the Impact of One Minute Resolution Magnetic Field Data

The continued difference in correlation between the rate of change of the magnetic field and GICs when the orientation of the strongest deflection is controlled for suggests that there is another effect present. We now assess the impact of down-sampling the magnetic signature to one-minute cadence, and how it may depend on the MLT of the observation. For this investigation we therefore require magnetic field data at a higher time resolution than 60 s. There are 1 s resolution data available for the EYR station from approximately 2010, which we use for this investigation. A total of 72 SCs have the required data. Figure 8a shows a Superposed Epoch Analysis (SEA) of the magnetic signatures observed during SCs, aligned to the epoch just prior to the largest increase in the field. Meanwhile, Figure 8b shows a histogram of the largest rate of change of the magnetic field (H') in each SC.

Inspecting Figure 8a, we can see that while there are a variety of different SC signatures, qualitatively some of the largest and fastest changes of the field are observed during the day, shown in orange. Those signatures observed during the night (in blue) commonly take between $1\frac{1}{2}$ to 3 minutes to rise to their maximum value. In contrast, those on the dayside have often completed their rise in less than one minute. The histogram in Figure 8b, while reducing each SC down to its most extreme rate of change, also shows a split between those observed during the day and at night. Of the 10 largest maximum H' observed, 8 were observed when EYR was on the dayside of the Earth. These results suggest that there is a diurnal variation in the rise-time of the SC signature, with those on the dayside showing a faster rising magnetic field signature. This difference could explain why dayside SCs appear to generate larger than expected GICs at the ISL M6 transformer in New Zealand.

We also find that the three events with maximum H' of over 200 nTmin^{-1} were all later classified as SSC-type events. This may suggest that highly geo-effective shocks, i.e. those which drive the most intense global magnetospheric response (geomagnetic storms) may also cause the most rapid initial magnetic field changes on the ground.

Recently, Clilverd et al. (2020) compared the frequency content of the magnetic field and GICs in New Zealand, during different intervals and with distinct magnetospheric drivers. They found that filtering the magnetic field with a running window of ± 2 minutes led to consistent spectral power profiles between the magnetic field and GICs. They suggested that using one minute averages for their data (i.e. 60 s resolution data) effec-

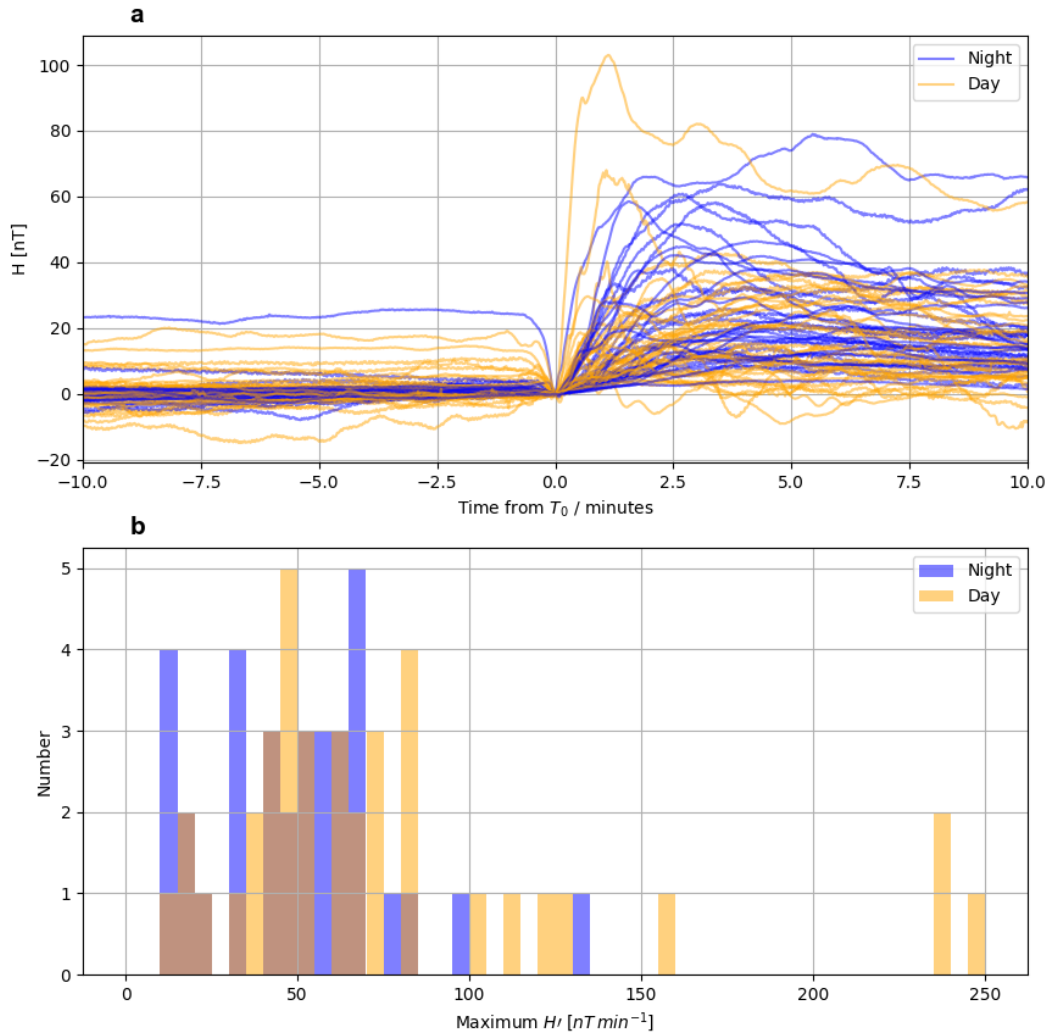


Figure 8. Assessing higher cadence magnetic field measurements. Top (a), Superposed Epoch Analysis (SEA) of the magnetic signature during 72 SCs, with the 38 observed on the dayside (0600-1800 MLT) in orange and the 34 on the nightside (1800 - 0600 MLT) in blue. Bottom (b), a histogram of the maximum rate of change of the magnetic field observed during each SC, with the colors as in (a). We note that overlapping bars result in a brown color.

427 tively compensated for the frequency dependence and any lags and inductance effects
428 in the comparison between magnetic field variations and GICs, at the location of their
429 study. This would also naturally explain the excellent correlations that have been ob-
430 served between 60 s resolution magnetic field and GIC data (e.g. Mac Manus et al., 2017).
431 However, in the current work we have shown that some of the scatter in the correlations
432 of the 60 s data can potentially be explained by information about the SC magnetic sig-
433 nature at sub-minute resolution, for the case of our nearly impulsive driver.

434 4.2 Implications for Space Weather Forecasting

435 Skillful models have been created that can forecast the ground magnetic field, based
436 on the incident solar wind. However, the timing and exact magnitude of the magnetic
437 field have proven difficult to predict precisely (Pulkkinen et al., 2013; Wintoft et al., 2015;
438 Keese et al., 2020). Re-framing the problem to predict the maximum magnetic rate of
439 change in a specific window of time has generally proven to be a result that can be fore-
440 cast with greater skill (e.g. Pulkkinen et al., 2013; Tóth et al., 2014; Smith, Forsyth, Rae,
441 Garton, et al., 2021). However, the results in this work reinforce the importance of de-
442 tailed local modeling for translating predicted rates of change of the magnetic field to
443 GICs, showing that a simple linear translation from the one-minute rate of change of the
444 magnetic field to GICs may be out by 30% (at the location of our study), even for the
445 simplest of magnetospheric signatures.

446 This work also highlights the importance of the local time of a location, even for
447 what is often considered a relatively simple, global and impulsive magnetic field change.
448 For the ISL M6 transformer in New Zealand, SCs that occur between MLTs of 0600 and
449 1800 appear to more effectively generate GICs, resulting in GICs that are $\sim 30\%$ larger
450 than might be found if the SC were to occur between MLTs of 1800 and 0600. We re-
451 mind the reader that for very narrow MLT windows (± 2 hours) this difference increased
452 to 60%. It seems quite reasonable that day/night GIC magnitude differences of this size
453 could control whether a given transformer suffers damage or does not; these findings re-
454 late to the hazard forecasting levels for power grid operators located at different MLT
455 for a given shock arrival, if provided with forecasts of the magnetic field.

456 Further, we have shown that those SCs that are followed by a geomagnetic storm,
457 i.e. SSCs (Curto et al., 2007), are associated with GIC magnitudes around 22% larger
458 than may be expected of those during isolated SCs. Recently, Smith et al. (2020) demon-
459 strated that we can forecast whether an observed interplanetary shock will be related
460 to an SSC or SI, based purely upon the solar wind immediately around the shock at L1.
461 In principle this would allow $\sim 30\text{--}60$ minutes of warning for ground power networks.
462 Our findings increase the value of such a forecast, which would provide key information
463 when attempting to quantify the space weather implications of an interplanetary shock
464 ahead of time.

465 We emphasize that our results are dependent upon the local geology and param-
466 eters of the power network on the South Island of New Zealand local to EYR/ISL: the
467 precise values quoted will not necessarily correspond with those that would be obtained
468 even for other transformers on the same network. Nonetheless, these results underscore
469 that the direction and sub-minute rate of change of the magnetic field are critical for the
470 estimation of GICs from magnetic field predictions. In general, this should hold true for
471 other locations across the globe, and neglect of these parameters may lead to discrep-
472 ancies of similar order (e.g. $\sim 30\%$ in this work for the EYR/ISL M6 locations). For
473 SCs, this will be particularly important at mid-latitudes where the magnitude of the SC
474 DL and DP components are both considerable, and therefore the orientation of SCs may
475 be more variable.

5 Summary

In this work we have investigated the relationship between the rate of change of the magnetic field and GICs during Sudden Commencements (SCs) at a location on New Zealand's South Island. We first showed excellent correspondence between one minute resolution rate of change of the magnetic field at EYR and GICs at ISL observed during SCs, with correlation coefficients of ~ 0.9 , confirming previously reported results (e.g. Mac Manus et al., 2017; Rodger et al., 2017).

We then showed that the gradient of the correlation between the rate of change of the magnetic field at EYR and GICs at ISL appears to be stronger during those SCs that are subsequently associated with a geomagnetic storm (SSCs). In this case, a given rate of change of the magnetic field is associated with a $\sim 22\%$ larger GIC at ISL, compared to those events for which no geomagnetic storm is later observed. Our work has demonstrated that the MLT of New Zealand is important when assessing the correlation of the rate of change of the magnetic field and GICs during SCs. If New Zealand is located on the dayside of the Earth then a given rate of change of the magnetic field observed at EYR is associated with a $\sim 30\%$ larger GIC at ISL.

We explored possible reasons behind the observed differences in correlation, assessing the impact of the orientation of the vector rate of change during the SC, as well as the impact of down-sampling the magnetic signature to 60 s. We showed that if the largest rate of change of the magnetic field within the SC was predominantly in the geographical east-west direction then a given rate of change of the magnetic field is associated with a 36% larger GIC. Further, when we controlled for the orientation of the rate of change of the magnetic field there was a residual effect, inflating the gradient of the correlation between the rate of change of the magnetic field and GICs on the dayside of the Earth. We used higher resolution (1 s cadence) data to demonstrate that SCs on the dayside may present with larger/faster rates of change of the magnetic field, with eight of the top 10 fastest deflections being found when New Zealand was on the dayside of the planet. We therefore conclude that both the orientation and properties of the SC signature found at sub-minute resolution are crucial when modeling the resulting GICs.

In terms of space weather forecasting, this suggests that predicting the magnitude of rate of change of the magnetic field is insufficient to precisely quantify resulting GICs, even during the relatively simple and impulsive SCs. Though the precise results of the study are specific to the local geology and network configuration, it is possible that the hazard to electrical networks at the arrival of an extreme shock event will depend on the MLT of the power network, with Sun-facing (i.e. noon MLTs) most severely exposed.

Appendix A More Limited Local Time Comparison

Acknowledgments

The results presented in this paper rely on the data collected at Eyrewell magnetometer station. We thank the Institute of Geological and Nuclear Sciences Limited (GNS) for supporting its operation, and INTERMAGNET for promoting high standards of magnetic observatory practice (www.intermagnet.org). The data were downloaded from <https://intermagnet.github.io> and are freely available there. The New Zealand electrical transmission network DC measurements were provided to us by Transpower New Zealand with caveats and restrictions. This includes requirements of permission before all publications and presentations and no ability to provide the observations themselves. Requests for access to these characteristics and the DC measurements need to be made to Transpower New Zealand. At this time the contact point is Michael Dalzell (Michael.Dalzell@transpower.co.nz).

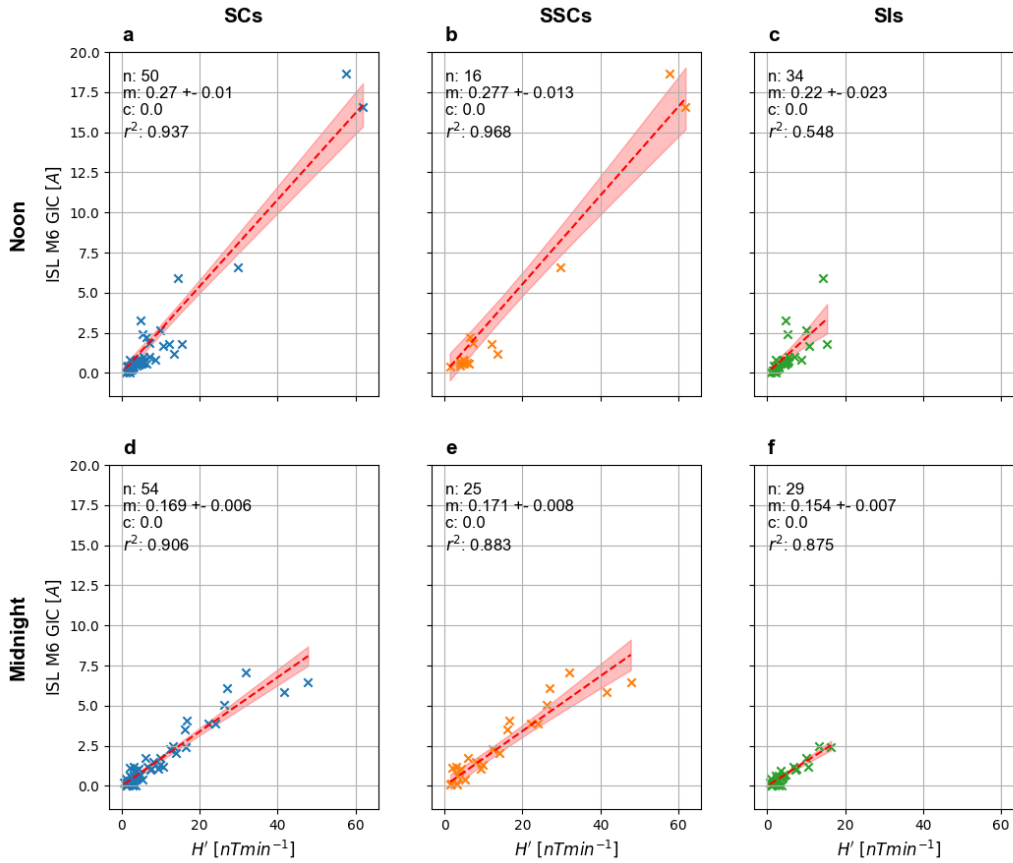


Figure A1. Scatter plots showing the correlation between H' at EYR and the GIC measured at ISL, split by the MLT of EYR during the SC. The top row (a - c) shows those events that occurred when EYR was near noon, i.e. between 1000 and 1400 MLT, while the bottom row (d - f) shows that occurred when EYR was on near midnight, i.e. between 2200 and 0200 MLT. The plots are shown for all SCs (a, d), SSCs (b, e) and SIs (c, f) that fall within the MLT bins. The format is the same as for Figure 3.

AWS and IJR were supported by STFC Consolidated Grant ST/S000240/1, and NERC grants NE/P017150/1 and NE/V002724/1. CJR and DHM supported by the New Zealand Ministry of Business, Innovation and Employment Endeavour Fund Research Programme contract UOOX2002. CF was supported by the NERC Independent Research Fellowship NE/N014480/1 and STFC Consolidated Grant ST/S000240/1.

References

- Akasofu, S.-I., & Chao, J. (1980, apr). Interplanetary shock waves and magnetospheric substorms. *Planetary and Space Science*, *28*(4), 381–385. Retrieved from <https://www.sciencedirect.com/science/article/pii/0032063380900422?via%3Dihub> doi: 10.1016/0032-0633(80)90042-2
- Araki, T. (1994, jan). A Physical Model of the Geomagnetic Sudden Commencement. In M. Engebretson, K. Takahashi, & M. Scholer (Eds.), *Solar wind sources of magnetospheric ultra-low-frequency waves* (p. 183).
- Bedrosian, P. A., & Love, J. J. (2015, dec). Mapping geoelectric fields during magnetic storms: Synthetic analysis of empirical United States impedances. *Geophysical Research Letters*, *42*(23), 10160–10170. Retrieved from <https://onlinelibrary.wiley.com/doi/abs/10.1002/2015GL066636> doi: 10.1002/2015GL066636
- Beggan, C. D. (2015, dec). Sensitivity of geomagnetically induced currents to varying auroral electrojet and conductivity models. *Earth, Planets and Space*, *67*(1), 24. Retrieved from <http://www.earth-planets-space.com/content/67/1/24> doi: 10.1186/s40623-014-0168-9
- Beggan, C. D., Beamish, D., Richards, A., Kelly, G. S., & Alan, A. W. (2013, jul). Prediction of extreme geomagnetically induced currents in the UK high-voltage network. *Space Weather*, *11*(7), 407–419. Retrieved from <https://onlinelibrary.wiley.com/doi/10.1002/swe.20065> doi: 10.1002/swe.20065
- Beland, J., & Small, K. (2004). Space weather effects on power transmission systems: The cases of Hydro-Quebec and transpower NewZealand Ltd [Proceedings Paper]. In I. Daglis (Ed.), *Effects of space weather on technology infrastructure* (Vol. 176, pp. 287–299). PO BOX 17, 3300 AA DORDRECHT, NETHERLANDS: SPRINGER.
- Blake, S. P., Gallagher, P. T., Campanyà, J., Hogg, C., Beggan, C. D., Thomson, A. W., ... Bell, D. (2018). A Detailed Model of the Irish High Voltage Power Network for Simulating GICs. *Space Weather*, *16*(11), 1770–1783. Retrieved from <https://doi.org/10.1029/2018SW001926> doi: 10.1029/2018SW001926
- Bolduc, L. (2002, nov). GIC observations and studies in the Hydro-Québec power system. *Journal of Atmospheric and Solar-Terrestrial Physics*, *64*(16), 1793–1802. Retrieved from <http://linkinghub.elsevier.com/retrieve/pii/S1364682602001281> doi: 10.1016/S1364-6826(02)00128-1
- Boteler, D. H. (2021, nov). Modeling Geomagnetic Interference on Railway Signaling Track Circuits. *Space Weather*, *19*(1). Retrieved from <https://onlinelibrary.wiley.com/doi/10.1029/2020SW002609> doi: 10.1029/2020SW002609
- Boteler, D. H., Pirjola, R. J., & Nevanlinna, H. (1998, jan). The effects of geomagnetic disturbances on electrical systems at the Earth's surface. *Advances in Space Research*, *22*(1), 17–27. Retrieved from <http://linkinghub.elsevier.com/retrieve/pii/S027311779701096X> doi: 10.1016/S0273-1177(97)01096-X
- Camporeale, E., Cash, M. D., Singer, H. J., Balch, C. C., Huang, Z., & Toth, G. (2020, oct). A gray-box model for a probabilistic estimate of regional ground magnetic perturbations: Enhancing the NOAA operational Geospace

- 576 model with machine learning. *Journal of Geophysical Research: Space*
 577 *Physics*. Retrieved from [https://onlinelibrary.wiley.com/doi/10.1029/](https://onlinelibrary.wiley.com/doi/10.1029/2019JA027684)
 578 [2019JA027684](https://onlinelibrary.wiley.com/doi/10.1029/2019JA027684) doi: 10.1029/2019JA027684
- 579 Carter, B. A., Pradipta, R., Zhang, K., Yizengaw, E., Halford, A. J., & Norman,
 580 R. (2015). Interplanetary shocks and the resulting geomagnetically induced
 581 currents at the equator. *Geophysical Research Letters*, *42*(16), 6554–6559.
 582 Retrieved from [https://agupubs.onlinelibrary.wiley.com/doi/pdf/](https://agupubs.onlinelibrary.wiley.com/doi/pdf/10.1002/2015GL065060)
 583 [10.1002/2015GL065060](https://agupubs.onlinelibrary.wiley.com/doi/pdf/10.1002/2015GL065060) doi: 10.1002/2015gl065060
- 584 Cash, M. D., Wrobel, J. S., Cosentino, K. C., & Reinard, A. A. (2014, jun). Char-
 585 acterizing interplanetary shocks for development and optimization of an auto-
 586 mated solar wind shock detection algorithm. *Journal of Geophysical Research:*
 587 *Space Physics*, *119*(6), 4210–4222. Retrieved from [http://doi.wiley.com/](http://doi.wiley.com/10.1002/2014JA019800)
 588 [10.1002/2014JA019800](http://doi.wiley.com/10.1002/2014JA019800) doi: 10.1002/2014JA019800
- 589 Clilverd, M. A., Rodger, C. J., Brundell, J. B., Dalzell, M., Martin, I., Mac Manus,
 590 D. H., ... Obana, Y. (2018, jun). Long-Lasting Geomagnetically Induced
 591 Currents and Harmonic Distortion Observed in New Zealand During the
 592 7–8 September 2017 Disturbed Period. *Space Weather*, *16*(6), 704–717.
 593 Retrieved from <http://doi.wiley.com/10.1029/2018SW001822> doi:
 594 [10.1029/2018SW001822](http://doi.wiley.com/10.1029/2018SW001822)
- 595 Clilverd, M. A., Rodger, C. J., Brundell, J. B., Dalzell, M., Martin, I., Mac Manus,
 596 D. H., & Thomson, N. R. (2020, oct). Geomagnetically Induced Currents and
 597 Harmonic Distortion: High Time Resolution Case Studies. *Space Weather*,
 598 *18*(10). Retrieved from [https://onlinelibrary.wiley.com/doi/10.1029/](https://onlinelibrary.wiley.com/doi/10.1029/2020SW002594)
 599 [2020SW002594](https://onlinelibrary.wiley.com/doi/10.1029/2020SW002594) doi: 10.1029/2020SW002594
- 600 Cordell, D., Unsworth, M. J., Lee, B., Haneson, C., Milling, D. K., & Mann,
 601 I. R. (2021, oct). Estimating the Geoelectric Field and Electric Power
 602 Transmission Line Voltage During a Geomagnetic Storm in Alberta, Canada
 603 Using Measured Magnetotelluric Impedance Data: The Influence of Three-
 604 Dimensional Electrical Structures in the Lithosphere. *Space Weather*, *19*(10),
 605 e2021SW002803. Retrieved from [https://onlinelibrary.wiley.com/doi/](https://onlinelibrary.wiley.com/doi/10.1029/2021SW002803)
 606 [10.1029/2021SW002803](https://onlinelibrary.wiley.com/doi/10.1029/2021SW002803) doi: 10.1029/2021SW002803
- 607 Curto, J. J., Araki, T., & Alberca, L. F. (2007, nov). Evolution of the con-
 608 cept of Sudden Storm Commencements and their operative identifica-
 609 tion. *Earth, Planets and Space*, *59*(11), i–xii. Retrieved from [http://](http://earth-planets-space.springeropen.com/articles/10.1186/BF03352059)
 610 earth-planets-space.springeropen.com/articles/10.1186/BF03352059
 611 doi: 10.1186/BF03352059
- 612 Dimmock, A. P., Rosenqvist, L., Hall, J. O., Viljanen, A., Yordanova, E., Honkonen,
 613 I., ... Sjöberg, E. C. (2019, jun). The GIC and Geomagnetic Response Over
 614 Fennoscandia to the 7–8 September 2017 Geomagnetic Storm. *Space Weather*,
 615 *17*(7), 989–1010. Retrieved from [https://onlinelibrary.wiley.com/doi/](https://onlinelibrary.wiley.com/doi/abs/10.1029/2018SW002132)
 616 [abs/10.1029/2018SW002132](https://onlinelibrary.wiley.com/doi/abs/10.1029/2018SW002132) doi: 10.1029/2018SW002132
- 617 Dimmock, A. P., Rosenqvist, L., Welling, D. T., Viljanen, A., Honkonen, I., Boyn-
 618 ton, R. J., & Yordanova, E. (2020, jun). On the Regional Variability of
 619 dB/dt and Its Significance to GIC. *Space Weather*, *18*(8). Retrieved from
 620 <https://onlinelibrary.wiley.com/doi/abs/10.1029/2020SW002497> doi:
 621 [10.1029/2020SW002497](https://onlinelibrary.wiley.com/doi/abs/10.1029/2020SW002497)
- 622 Divett, T., Mac Manus, D. H., Richardson, G. S., Beggan, C. D., Rodger, C. J., Ing-
 623 ham, M., ... Obana, Y. (2020, jun). Geomagnetically Induced Current Model
 624 Validation From New Zealand’s South Island. *Space Weather*, *18*(8). Retrieved
 625 from <https://onlinelibrary.wiley.com/doi/abs/10.1029/2020SW002494>
 626 doi: 10.1029/2020SW002494
- 627 Divett, T., Richardson, G. S., Beggan, C. D., Rodger, C. J., Boteler, D. H., Ingham,
 628 M., ... Dalzell, M. (2018, jun). Transformer-Level Modeling of Geomagneti-
 629 cally Induced Currents in New Zealand’s South Island. *Space Weather*, *16*(6),
 630 718–735. Retrieved from <http://doi.wiley.com/10.1029/2018SW001814>

- 631 doi: 10.1029/2018SW001814
- 632 Eastwood, J. P., Mistry, R., Phan, T. D., Schwartz, S. J., Ergun, R. E., Drake,
633 J. F., ... Russell, C. T. (2018, apr). Guide field reconnection: exhaust struc-
634 ture and heating. *Geophysical Research Letters*. Retrieved from [http://](http://doi.wiley.com/10.1029/2018GL077670)
635 doi.wiley.com/10.1029/2018GL077670 doi: 10.1029/2018GL077670
- 636 Eastwood, J. P., Nakamura, R., Turc, L., Mejnertsen, L., & Hesse, M. (2017,
637 aug). *The Scientific Foundations of Forecasting Magnetospheric Space*
638 *Weather* (Vol. 212) (No. 3-4). Springer Netherlands. Retrieved from
639 <http://link.springer.com/10.1007/s11214-017-0399-8> doi: 10.1007/
640 s11214-017-0399-8
- 641 Fiori, R. A. D., Boteler, D. H., & Gillies, D. M. (2014, jan). Assessment of GIC risk
642 due to geomagnetic sudden commencements and identification of the current
643 systems responsible. *Space Weather*, 12(1), 76–91. Retrieved from [http://](http://doi.wiley.com/10.1002/2013SW000967)
644 doi.wiley.com/10.1002/2013SW000967 doi: 10.1002/2013SW000967
- 645 Forsyth, C., Watt, C. E. J., Rae, I. J., Fazakerley, A. N., Kalmoni, N. M. E., Free-
646 man, M. P., ... Carr, C. M. (2014, dec). Increases in plasma sheet temper-
647 ature with solar wind driving during substorm growth phases. *Geophysical*
648 *Research Letters*, 41(24), 8713–8721. Retrieved from [http://doi.wiley.com/](http://doi.wiley.com/10.1002/2014GL062400)
649 [10.1002/2014GL062400](http://doi.wiley.com/10.1002/2014GL062400) doi: 10.1002/2014GL062400
- 650 Freeman, M. P., Forsyth, C., & Rae, I. J. (2019, may). The influence of
651 substorms on extreme rates of change of the surface horizontal mag-
652 netic field in the U.K. *Space Weather*, 2018SW002148. Retrieved from
653 <https://onlinelibrary.wiley.com/doi/abs/10.1029/2018SW002148> doi:
654 10.1029/2018SW002148
- 655 Friis-Christensen, E., McHenry, M. A., Clauer, C. R., & Vennerstrøm, S. (1988,
656 mar). Ionospheric traveling convection vortices observed near the polar cleft: A
657 triggered response to sudden changes in the solar wind. *Geophysical Research*
658 *Letters*, 15(3), 253–256. Retrieved from [http://doi.wiley.com/10.1029/](http://doi.wiley.com/10.1029/GL015i003p00253)
659 [GL015i003p00253](http://doi.wiley.com/10.1029/GL015i003p00253) doi: 10.1029/GL015i003p00253
- 660 Gaunt, C. T., & Coetzee, G. (2007). Transformer failures in regions incorrectly con-
661 sidered to have low GIC-risk. In *2007 IEEE Lausanne PowerTech, Proceedings* (pp.
662 807–812). doi: 10.1109/PCT.2007.4538419
- 663 Gonzalez, W. D., Joselyn, J. A., Kamide, Y., Kroehl, H. W., Ros, G., Tsuru, B. T.,
664 & Vasyliunas, V. M. (1994). *What is a geomagnetic storm?* (Vol. 99; Tech.
665 Rep. No. A4). Retrieved from [https://agupubs.onlinelibrary.wiley.com/](https://agupubs.onlinelibrary.wiley.com/doi/pdf/10.1029/93JA02867)
666 [doi/pdf/10.1029/93JA02867](https://agupubs.onlinelibrary.wiley.com/doi/pdf/10.1029/93JA02867) doi: 10.1029/93JA02867
- 667 Kappenman, J. G. (2003, dec). Storm sudden commencement events and the
668 associated geomagnetically induced current risks to ground-based systems
669 at low-latitude and midlatitude locations. *Space Weather*, 1(3), n/a–n/a.
670 Retrieved from <http://doi.wiley.com/10.1029/2003SW000009> doi:
671 10.1029/2003sw000009
- 672 Kappenman, J. G. (2005). An overview of the impulsive geomagnetic field dis-
673 turbances and power grid impacts associated with the violent Sun-Earth
674 connection events of 29-31 October 2003 and a comparative evaluation with
675 other contemporary storms. *Space Weather*, 3(8). Retrieved from [https://](https://agupubs.onlinelibrary.wiley.com/doi/pdf/10.1029/2004SW000128)
676 agupubs.onlinelibrary.wiley.com/doi/pdf/10.1029/2004SW000128 doi:
677 10.1029/2004SW000128
- 678 Keese, A. M., Pinto, V., Coughlan, M., Lennox, C., Mahmud, M. S., & Con-
679 nor, H. K. (2020, oct). Comparison of Deep Learning Techniques to
680 Model Connections Between Solar Wind and Ground Magnetic Perturba-
681 tions. *Frontiers in Astronomy and Space Sciences*, 7, 72. Retrieved from
682 <https://www.frontiersin.org/article/10.3389/fspas.2020.550874/full>
683 doi: 10.3389/fspas.2020.550874
- 684 Kokubun, S. (1983, dec). Characteristics of storm sudden commencement at geo-
685 stationary orbit. *Journal of Geophysical Research*, 88(A12), 10025. Re-

- 686 trieved from <http://doi.wiley.com/10.1029/JA088iA12p10025> doi:
687 10.1029/JA088iA12p10025
- 688 Liu, L., Ge, X., Zong, W., Zhou, Y., & Liu, M. (2016, oct). Analysis of the moni-
689 toring data of geomagnetic storm interference in the electrification system of a
690 high-speed railway. *Space Weather*, *14*(10), 754–763. Retrieved from [http://](http://doi.wiley.com/10.1002/2016SW001411)
691 doi.wiley.com/10.1002/2016SW001411 doi: 10.1002/2016SW001411
- 692 Lühr, H., Schlegel, K., Araki, T., Rother, M., & Förster, M. (2009, may). Night-time
693 sudden commencements observed by CHAMP and ground-based magnetome-
694 ters and their relationship to solar wind parameters. *Annales Geophysicae*,
695 *27*(5), 1897–1907. Retrieved from [https://www.ann-geophys.net/27/1897/](https://www.ann-geophys.net/27/1897/2009/)
696 2009/ doi: 10.5194/angeo-27-1897-2009
- 697 Mac Manus, D. H., Rodger, C. J., Dalzell, M., Thomson, A. W. P., Clilverd,
698 M. A., Petersen, T., ... Divett, T. (2017, aug). Long-term geomagnet-
699 ically induced current observations in New Zealand: Earth return correc-
700 tions and geomagnetic field driver. *Space Weather*, *15*(8), 1020–1038.
701 Retrieved from <http://doi.wiley.com/10.1002/2017SW001635> doi:
702 10.1002/2017SW001635
- 703 Mac Manus, D. H., Rodger, C. J., Ingham, M., Clilverd, M. A., Dalzell, M., Di-
704 vett, T., ... Petersen, T. (2022). Geomagnetically Induced Current Model
705 in New Zealand across Multiple Disturbances: Validation and Extension to
706 non-Monitored Transformers. *Space Weather*, *20*. doi: e2021SW002955
- 707 Marshall, R. A., Dalzell, M., Waters, C. L., Goldthorpe, P., & Smith, E. A. (2012,
708 aug). Geomagnetically induced currents in the New Zealand power network.
709 *Space Weather*, *10*(8), n/a–n/a. Retrieved from [http://doi.wiley.com/10](http://doi.wiley.com/10.1029/2012SW000806)
710 .1029/2012SW000806 doi: 10.1029/2012SW000806
- 711 Mayaud, P. N. (1973). A hundred year series of geomagnetic data, 1868-1967: in-
712 dices aa, storm sudden commencements(SSC). *IUGG Publ. Office*, 256.
- 713 Moretto, T., Friis-Christensen, E., Lühr, H., & Zesta, E. (1997, jun). Global
714 perspective of ionospheric traveling convection vortices: Case studies of
715 two Geospace Environmental Modeling events. *Journal of Geophysic-
716 al Research: Space Physics*, *102*(A6), 11597–11610. Retrieved from
717 <http://doi.wiley.com/10.1029/97JA00324> doi: 10.1029/97JA00324
- 718 Murphy, K. R., Mann, I. R., Rae, I. J., Waters, C. L., Frey, H. U., Kale, A., ... Ko-
719 rth, H. (2013, dec). The detailed spatial structure of field-aligned currents
720 comprising the substorm current wedge. *Journal of Geophysical Research:
721 Space Physics*, *118*(12), 7714–7727. Retrieved from [http://doi.wiley.com/](http://doi.wiley.com/10.1002/2013JA018979)
722 10.1002/2013JA018979 doi: 10.1002/2013JA018979
- 723 Ngwira, C. M., Pulkkinen, A. A., Bernabeu, E., Eichner, J., Viljanen, A., &
724 Crowley, G. (2015, sep). Characteristics of extreme geoelectric fields
725 and their possible causes: Localized peak enhancements. *Geophysical Re-
726 search Letters*, *42*(17), 6916–6921. Retrieved from [https://agupubs](https://agupubs.onlinelibrary.wiley.com/doi/full/10.1002/2015GL065061)
727 .onlinelibrary.wiley.com/doi/full/10.1002/2015GL065061%4010.1002/
728 %28ISSN%291542-7390.GIC15 doi: 10.1002/2015GL065061
- 729 Ngwira, C. M., Sibeck, D., Silveira, M. V. D., Georgiou, M., Weygand, J. M.,
730 Nishimura, Y., & Hampton, D. (2018, jun). A Study of Intense Local
731 d $j_{\parallel} B_{\parallel} / i_{\parallel} / d j_{\parallel} t_{\parallel} / i_{\parallel}$ Variations During Two Geomagnetic Storms. *Space
732 Weather*, *16*(6), 676–693. Retrieved from [http://doi.wiley.com/10.1029/](http://doi.wiley.com/10.1029/2018SW001911)
733 2018SW001911 doi: 10.1029/2018SW001911
- 734 Oliveira, D., & Samsonov, A. (2018, jan). Geoeffectiveness of interplanetary shocks
735 controlled by impact angles: A review. *Advances in Space Research*, *61*(1), 1–
736 44. Retrieved from [https://www.sciencedirect.com/science/article/pii/](https://www.sciencedirect.com/science/article/pii/S0273117717307275?via%3Dihub)
737 S0273117717307275?via%3Dihub doi: 10.1016/J.ASR.2017.10.006
- 738 Oliveira, D. M., Arel, D., Raeder, J., Zesta, E., Ngwira, C. M., Carter, B. A., ...
739 Gjerloev, J. W. (2018, jun). Geomagnetically Induced Currents Caused
740 by Interplanetary Shocks With Different Impact Angles and Speeds. *Space*

- 741 *Weather*, 16(6), 636–647. Retrieved from [http://doi.wiley.com/10.1029/](http://doi.wiley.com/10.1029/2018SW001880)
742 2018SW001880 doi: 10.1029/2018SW001880
- 743 Oughton, E. J., Hapgood, M., Richardson, G. S., Beggan, C. D., Thomson, A. W.,
744 Gibbs, M., ... Horne, R. B. (2019, may). A Risk Assessment Framework for
745 the Socioeconomic Impacts of Electricity Transmission Infrastructure Failure
746 Due to Space Weather: An Application to the United Kingdom. *Risk Analysis*,
747 39(5), 1022–1043. Retrieved from [https://onlinelibrary.wiley.com/doi/](https://onlinelibrary.wiley.com/doi/abs/10.1111/risa.13229)
748 [abs/10.1111/risa.13229](https://onlinelibrary.wiley.com/doi/abs/10.1111/risa.13229) doi: 10.1111/risa.13229
- 749 Pulkkinen, A., Bernabeu, E., Eichner, J., Viljanen, A., & Ngwira, C. (2015, dec).
750 Regional-scale high-latitude extreme geoelectric fields pertaining to geomag-
751 netically induced currents. *Earth, Planets and Space*, 67(1), 93. Retrieved
752 from <http://www.earth-planets-space.com/content/67/1/93> doi:
753 10.1186/s40623-015-0255-6
- 754 Pulkkinen, A., Lindahl, S., Viljanen, A., & Pirjola, R. (2005, aug). Geomagnetic
755 storm of 29–31 October 2003: Geomagnetically induced currents and their rela-
756 tion to problems in the Swedish high-voltage power transmission system. *Space*
757 *Weather*, 3(8), n/a–n/a. Retrieved from [http://doi.wiley.com/10.1029/](http://doi.wiley.com/10.1029/2004SW000123)
758 2004SW000123 doi: 10.1029/2004SW000123
- 759 Pulkkinen, A., Rastätter, L., Kuznetsova, M., Singer, H., Balch, C., Weimer,
760 D., ... Weigel, R. (2013, jun). Community-wide validation of geospace
761 model ground magnetic field perturbation predictions to support model
762 transition to operations. *Space Weather*, 11(6), 369–385. Retrieved from
763 <http://doi.wiley.com/10.1002/swe.20056> doi: 10.1002/swe.20056
- 764 Rajput, V. N., Boteler, D. H., Rana, N., Saiyed, M., Anjana, S., & Shah, M.
765 (2020, nov). Insight into impact of geomagnetically induced currents on
766 power systems: Overview, challenges and mitigation. *Electric Power Sys-*
767 *tems Research*, 106927. Retrieved from [https://www.sciencedirect.com/](https://www.sciencedirect.com/science/article/pii/S0378779620307252?casa_token=Qs4jRHozhEkAAAAA:4AV7P1SDLxVc7NkeV0hvhPk0qJfGvgoONrejBL7VLzYer8fpctmlt2uGLtyVZsclpebG_U-imEi6)
768 [science/article/pii/S0378779620307252?casa_token=Qs4jRHozhEkAAAAA:](https://www.sciencedirect.com/science/article/pii/S0378779620307252?casa_token=Qs4jRHozhEkAAAAA:4AV7P1SDLxVc7NkeV0hvhPk0qJfGvgoONrejBL7VLzYer8fpctmlt2uGLtyVZsclpebG_U-imEi6)
769 [4AV7P1SDLxVc7NkeV0hvhPk0qJfGvgoONrejBL7VLzYer8fpctmlt2uGLtyVZsclpebG](https://www.sciencedirect.com/science/article/pii/S0378779620307252?casa_token=Qs4jRHozhEkAAAAA:4AV7P1SDLxVc7NkeV0hvhPk0qJfGvgoONrejBL7VLzYer8fpctmlt2uGLtyVZsclpebG_U-imEi6)
770 [_U-imEi6](https://www.sciencedirect.com/science/article/pii/S0378779620307252?casa_token=Qs4jRHozhEkAAAAA:4AV7P1SDLxVc7NkeV0hvhPk0qJfGvgoONrejBL7VLzYer8fpctmlt2uGLtyVZsclpebG_U-imEi6) doi: 10.1016/J.EPSR.2020.106927
- 771 Rodger, C. J., Clilverd, M. A., Mac Manus, D. H., Martin, I., Dalzell, M.,
772 Brundell, J. B., ... Watson, N. R. (2020, mar). Geomagnetically In-
773 duced Currents and Harmonic Distortion: Storm-Time Observations From
774 New Zealand. *Space Weather*, 18(3), e2019SW002387. Retrieved from
775 <https://onlinelibrary.wiley.com/doi/abs/10.1029/2019SW002387> doi:
776 10.1029/2019SW002387
- 777 Rodger, C. J., Mac Manus, D. H., Dalzell, M., Thomson, A. W. P., Clarke, E.,
778 Petersen, T., ... Divett, T. (2017, nov). Long-Term Geomagnetically In-
779 duced Current Observations From New Zealand: Peak Current Estimates
780 for Extreme Geomagnetic Storms. *Space Weather*, 15(11), 1447–1460.
781 Retrieved from <http://doi.wiley.com/10.1002/2017SW001691> doi:
782 10.1002/2017SW001691
- 783 Rogers, N. C., Wild, J. A., Eastoe, E. F., Gjerloev, J. W., & Thomson, A. W. P.
784 (2020, feb). A global climatological model of extreme geomagnetic field
785 fluctuations. *Journal of Space Weather and Space Climate*, 10, 5. Re-
786 trieved from <https://www.swsc-journal.org/10.1051/swsc/2020008> doi:
787 10.1051/swsc/2020008
- 788 Russell, C. T., Ginskey, M., Petrincic, S., & Le, G. (1992, jun). The effect of
789 solar wind dynamic pressure changes on low and mid-latitude magnetic
790 records. *Geophysical Research Letters*, 19(12), 1227–1230. Retrieved from
791 <http://doi.wiley.com/10.1029/92GL01161> doi: 10.1029/92GL01161
- 792 Smith, A. W., Forsyth, C., Rae, I. J., Garton, T. M., Bloch, T., Jackman, C. M.,
793 & Bakrania, M. (2021, aug). Forecasting the Probability of Large
794 Rates of Change of the Geomagnetic Field in the UK: Timescales, Hori-
795 zons and Thresholds. *Space Weather*, e2021SW002788. Retrieved from

- 796 <https://onlinelibrary.wiley.com/doi/10.1029/2021SW002788> doi:
797 10.1029/2021SW002788
- 798 Smith, A. W., Forsyth, C., Rae, J., Rodger, C. J., & Freeman, M. P. (2021,
799 jun). The Impact of Sudden Commencements on Ground Magnetic Field
800 Variability: Immediate and Delayed Consequences. *Space Weather*, *19*(7),
801 e2021SW002764. Retrieved from [https://onlinelibrary.wiley.com/doi/](https://onlinelibrary.wiley.com/doi/10.1029/2021SW002764)
802 [10.1029/2021SW002764](https://onlinelibrary.wiley.com/doi/10.1029/2021SW002764) doi: 10.1029/2021SW002764
- 803 Smith, A. W., Freeman, M. P., Rae, I. J., & Forsyth, C. (2019, nov). The Influence
804 of Sudden Commencements on the Rate of Change of the Surface Horizontal
805 Magnetic Field in the United Kingdom. *Space Weather*, 2019SW002281.
806 Retrieved from [https://onlinelibrary.wiley.com/doi/abs/10.1029/](https://onlinelibrary.wiley.com/doi/abs/10.1029/2019SW002281)
807 [2019SW002281](https://onlinelibrary.wiley.com/doi/abs/10.1029/2019SW002281) doi: 10.1029/2019SW002281
- 808 Smith, A. W., Rae, I. J., Forsyth, C., Oliveira, D. M., Freeman, M. P., & Jackson,
809 D. R. (2020, nov). Probabilistic Forecasts of Storm Sudden Commence-
810 ments From Interplanetary Shocks Using Machine Learning. *Space Weather*,
811 *18*(11). Retrieved from [https://onlinelibrary.wiley.com/doi/10.1029/](https://onlinelibrary.wiley.com/doi/10.1029/2020SW002603)
812 [2020SW002603](https://onlinelibrary.wiley.com/doi/10.1029/2020SW002603) doi: 10.1029/2020SW002603
- 813 Southwood, D. J., & Kivelson, M. G. (1990, mar). The magnetohydrodynamic re-
814 sponse of the magnetospheric cavity to changes in solar wind pressure. *Jour-*
815 *nal of Geophysical Research*, *95*(A3), 2301. Retrieved from [http://doi.wiley](http://doi.wiley.com/10.1029/JA095iA03p02301)
816 [.com/10.1029/JA095iA03p02301](http://doi.wiley.com/10.1029/JA095iA03p02301) doi: 10.1029/JA095iA03p02301
- 817 Takeuchi, T., Araki, T., Viljanen, A., & Watermann, J. (2002, jul). Geomagnetic
818 negative sudden impulses: Interplanetary causes and polarization distribution.
819 *Journal of Geophysical Research*, *107*(A7), 1096. Retrieved from [http://](http://doi.wiley.com/10.1029/2001JA900152)
820 doi.wiley.com/10.1029/2001JA900152 doi: 10.1029/2001JA900152
- 821 Thomson, A. W., Dawson, E. B., & Reay, S. J. (2011, oct). Quantifying extreme be-
822 havior in geomagnetic activity. *Space Weather*, *9*(10). Retrieved from [http://](http://doi.wiley.com/10.1029/2011SW000696)
823 doi.wiley.com/10.1029/2011SW000696 doi: 10.1029/2011SW000696
- 824 Thomson, A. W., McKay, A. J., Clarke, E., & Reay, S. J. (2005, nov). Surface
825 electric fields and geomagnetically induced currents in the Scottish Power grid
826 during the 30 October 2003 geomagnetic storm. *Space Weather*, *3*(11), n/a–
827 n/a. Retrieved from <http://doi.wiley.com/10.1029/2005SW000156> doi:
828 [10.1029/2005SW000156](http://doi.wiley.com/10.1029/2005SW000156)
- 829 Tóth, G., Meng, X., Gombosi, T. I., & Rastätter, L. (2014, jan). Predicting the time
830 derivative of local magnetic perturbations. *Journal of Geophysical Research:*
831 *Space Physics*, *119*(1), 310–321. Retrieved from [http://doi.wiley.com/10](http://doi.wiley.com/10.1002/2013JA019456)
832 [.1002/2013JA019456](http://doi.wiley.com/10.1002/2013JA019456) doi: 10.1002/2013JA019456
- 833 Tsurutani, B. T., & Hajra, R. (2021, mar). The Interplanetary and Magnetospheric
834 causes of Geomagnetically Induced Currents (GICs) \geq 10 A in the Mäntsälä
835 Finland Pipeline: 1999 through 2019. *Journal of Space Weather and Space*
836 *Climate*, *11*, 23. Retrieved from [https://www.swsc-journal.org/10.1051/](https://www.swsc-journal.org/10.1051/swsc/2021001)
837 [swsc/2021001](https://www.swsc-journal.org/10.1051/swsc/2021001) doi: 10.1051/swsc/2021001
- 838 Viljanen, A., Nevanlinna, H., Pajunpää, K., & Pulkkinen, A. (2001). Time deriva-
839 tive of the horizontal geomagnetic field as an activity indicator. *Annales Geo-*
840 *physicae*, *19*(9), 1107–1118. Retrieved from [http://www.ann-geophys.net/](http://www.ann-geophys.net/19/1107/2001/)
841 [19/1107/2001/](http://www.ann-geophys.net/19/1107/2001/) doi: 10.5194/angeo-19-1107-2001
- 842 Viljanen, A., Pirjola, R., Prácer, E., Ahmadzai, S., & Singh, V. (2013). Geo-
843 magnetically induced currents in Europe: Characteristics based on a lo-
844 cal power grid model. *Space Weather*, *11*(10), 575–584. Retrieved from
845 <http://real.mtak.hu/2957/> doi: 10.1002/swe.20098
- 846 Wintoft, P., Wik, M., & Viljanen, A. (2015, mar). Solar wind driven empirical
847 forecast models of the time derivative of the ground magnetic field. *Journal of*
848 *Space Weather and Space Climate*, *5*, A7. Retrieved from [http://www.swsc](http://www.swsc-journal.org/10.1051/swsc/2015008)
849 [-journal.org/10.1051/swsc/2015008](http://www.swsc-journal.org/10.1051/swsc/2015008) doi: 10.1051/swsc/2015008
- 850 Yue, C., Zong, Q. G., Zhang, H., Wang, Y. F., Yuan, C. J., Pu, Z. Y., ... Wang,

- 851 C. R. (2010, may). Geomagnetic activity triggered by interplanetary
852 shocks. *Journal of Geophysical Research: Space Physics*, *115*(A5), n/a–
853 n/a. Retrieved from <http://doi.wiley.com/10.1029/2010JA015356> doi:
854 10.1029/2010JA015356
- 855 Zhang, J. J., Wang, C., Sun, T. R., Liu, C. M., & Wang, K. R. (2015, oct). GIC
856 due to storm sudden commencement in low-latitude high-voltage power net-
857 work in China: Observation and simulation. *Space Weather*, *13*(10), 643–
858 655. Retrieved from <http://doi.wiley.com/10.1002/2015SW001263> doi:
859 10.1002/2015SW001263
- 860 Zhang, J. J., Yu, Y. Q., Wang, C., Du, D., Wei, D., & Liu, L. G. (2020, aug). Mea-
861 surements and Simulations of the Geomagnetically Induced Currents in Low-
862 Latitude Power Networks During Geomagnetic Storms. *Space Weather*, *18*(8).
863 Retrieved from [https://onlinelibrary.wiley.com/doi/abs/10.1029/](https://onlinelibrary.wiley.com/doi/abs/10.1029/2020SW002549)
864 [2020SW002549](https://onlinelibrary.wiley.com/doi/abs/10.1029/2020SW002549) doi: 10.1029/2020SW002549
- 865 Zhou, X., & Tsurutani, B. T. (2001, sep). Interplanetary shock triggering of
866 nightside geomagnetic activity: Substorms, pseudobreakups, and quiescent
867 events. *Journal of Geophysical Research: Space Physics*, *106*(A9), 18957–
868 18967. Retrieved from <http://doi.wiley.com/10.1029/2000JA003028> doi:
869 10.1029/2000JA003028